



Fast Evaluation of Caprock Strength Sensitivity to Different CO₂ Solutions Using Small Sample Techniques

Laura Edvardsen¹ · Mohammad H. Bhuiyan¹ · Pierre R. Cerasi¹ · Ruben Bjørge¹

Received: 21 December 2020 / Accepted: 23 August 2021 / Published online: 16 September 2021
© The Author(s) 2021

Abstract

The Draupne shale is a rock formation functioning as overburden for gas reservoirs in the Norwegian Sea and potentially as caprock for future CO₂ storage locations as well. In this paper, the Draupne shale was exposed to several fluids: CO₂ gas, supercritical CO₂, CO₂ gas dissolved in brine, supercritical CO₂ dissolved in brine, as well as brine and dry air. The motivation for the exposure tests was to investigate whether injected CO₂ in a reservoir coming into contact with the caprock could change the caprock's mechanical properties and increase the risk for leakage of the stored CO₂. In addition, a systematic exposure study will provide more insight into the various processes susceptible of altering the shale's shear strength and acoustic velocity, such as clay hydration, mineral dissolution, and capillary forces. Due to the low permeability of the shale, experiments were conducted on mm-sized disk samples, reducing fluid diffusion into the shale, and allowing for many repeated tests on disks close by in the original core. The punch method, where a small circle is punched out of the shale, was used to assess shear strength, while continuous wave technique was used to assess ultrasonic velocity. Results show that the shale is not noticeably sensitive to CO₂, in the sense that no additional weakening is observed in the presence of CO₂ as compared to brine exposure. This last weakening effect is probably due to poor matching between pore fluid salinity and exposure brine strength.

Keywords CO₂ storage · Shale caprock · Shale strength · Shear strength

1 Introduction

Carbon dioxide (CO₂) capture and storage is considered an indispensable mitigation action to reduce the atmospheric emissions of CO₂ from human activities, if the Paris agreement goals are to be reached (Masson-Delmotte et al. 2018; Rubin and De Coninck 2005). Geological storage of CO₂ involves CO₂ injection into reservoir formations with high permeability, to sequester as large volumes as possible per storage site. To keep the CO₂ underground, the reservoir needs a low permeability caprock formation to serve as a seal (Busch et al. 2010). Loss of containment of the stored CO₂ is connected to the integrity of the sealing caprock; integrity can be lost as a consequence of too high increase in the reservoir pore pressure and accompanying stress changes in the caprock, or stress concentration reactivating

faults traversing reservoir and caprock (Rongved and Cerasi 2019). An ideal caprock is a non-fractured, non-permeable, non-porous formation that is also non-reactive with the surrounding fluids. Unfortunately, such a caprock does not exist. During geological storage of CO₂, the buoyant fluid will migrate upwards, forming a plume beneath the caprock. Through diffusion processes, CO₂ could migrate into the water-saturated pore space of the caprock (Song and Zhang 2013). This poses risks as the migrated CO₂ could alter the chemical, physical and mechanical properties of the caprock, again leading to lost integrity (Bhuiyan et al. 2020). Much research has been conducted to investigate the effect of CO₂ and CO₂-brine solution on shale strength, mostly in terms of UCS (unconfined compressive strength) and Young's Modulus. A reduction of shale strength upon exposure to gaseous and supercritical CO₂ have been confirmed by e.g., Al-Ameri et al. 2016 and Zhang et al. 2017. Dewhurst et al. 2020 reported an increase of strength and stiffness of the mudrock and expressed the importance of non-native pore fluids effect on shale integrity. Reduction of shale strength has been measured by several authors for shale saturated

✉ Laura Edvardsen
laura.edvardsen@sintef.no

¹ SINTEF Industry, Trondheim, Norway

with CO₂-saturated brine solution over various ranges of durations (e.g., Lyu et al. 2016; Agofack et al. 2019). Bhuiyan et al. 2020 summarized the processes occurring in shale upon exposure to dry CO₂ and brine -saturated CO₂ (both gaseous and supercritical). The processes occurring during exposure to dry CO₂ are drying, precipitation of minerals, adsorption of minerals, dissolution of organic matter, swelling and shrinkage of clay. Exposure to brine saturated CO₂ solution can result in dissolution of minerals, precipitation and reprecipitation of minerals and swelling/shrinkage of clays. These processes can lead to a change in composition, microstructure, and mechanical properties of the shale.

In this study, we tried to elaborate on the existing understanding of the processes by exposing a preserved shale (Draupne shale) to fluids at different conditions. Exposing the shale samples to air (dried) as well as to dry CO₂ (both gaseous and supercritical) can help to understand the effect of drying and separate the effect of other processes (e.g., sorption). Samples were exposed only to brine to investigate the resulting effect on the shale (mostly softening) compared to reference samples (preserved samples without exposure to any fluid) and dry samples. Samples were also exposed to CO₂-saturated brine (both gaseous and supercritical CO₂) to investigate the effect of pH. In addition to increased comprehension of the exposure effects, the different conditions of humidity and pH of the CO₂ solutions may have relevance for how far the injected CO₂ has travelled prior to reaching the shale caprock. Most CO₂ storage operations will involve injection of dry supercritical CO₂, such that with time, an increasing region near the injection well will be dried out and dry CO₂ may encounter the shale caprock as the plume rises alongside the well. However, as CO₂ penetrates further out in the reservoir, it will pick up resident brine and may at some point also come out of solution or at least not be in the supercritical state if pressure and temperature conditions change, especially after injection stop. Thus, other parts of the caprock may be in contact with wet CO₂, or dry CO₂ may suck out brine from the caprock shale. CO₂ migration in the reservoir is further detailed below.

1.1 Shale Strength Testing

The strength of rocks and other porous materials is compromised whenever the effective stresses exceed an intrinsic resistance of the material, either in tension or in compression (Fjar et al. 2008). The isotropic pressure of the pore space fluid counteracts the forces on the grain framework if these are compressive, potentially leading to tensile fracturing, when exceeding the tensile cementation limit (Cosgrove 1995). On the other hand, lowering too much the pore pressure may lead to shear fracturing of the grain cementation. In extreme cases, grain crushing can set in Zhang et al. (1990). It is usual to measure tensile and compressive shear strength

of rocks in the laboratory using standard procedures and sizes for the tested specimens. For tensile strength, Brazilian indirect testing on 1.5 in diameter disks is performed (Briševac et al. 2015), while for shear strength, axial compression is performed on 3 in long cylindrical core plugs (1 or 1.5 in diameter). Since shale rocks are fine-grained, the size needed to perform these tests can be somewhat reduced without affecting the results (Nes et al. 2004). Shear strength testing can thus be performed on 15 mm diameter times 30 mm long cylinder plugs, which is an advantage in terms of test duration, as these compression tests should not be performed faster than the pore fluid pressure can equilibrate. However, when exposing the shale to an external fluid, its permeability, typically in the nD range, still makes for long diffusion times for the fluid to fully penetrate the pore space. Reducing the sample even further, to a 15 mm diameter, 3–5 mm thick disk allows for quicker exposure to fluids, while still allowing for shear strength testing, using the punch method described below, in the experimental section.

1.2 Shale and CO₂ Interactions

When CO₂ is injected into a reservoir it can cause an evaporation of pore fluid water (Ott et al. 2011), be dissolved in the pore fluid (Greenwood and Earnshaw 2012), or remain as a separate phase of CO₂ that can migrate towards the caprock due to buoyancy forces or be trapped in the pore space of the reservoir rock (Benson and Cole 2008). The first event can cause salt precipitation in the reservoir rock which can lead to clogging and injectivity problems (Ott et al. 2011). The two latter events can directly affect the caprock.

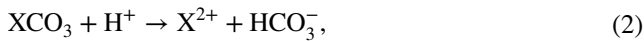
The magnitude of the buoyancy forces driving CO₂ upwards depends on the liquid already present in the reservoir (Kovscek 2002), while the shape of the CO₂ plume is affected by the formation heterogeneity (Flett et al. 2005). As the CO₂ migrates through the reservoir matrix, some of it will be trapped in the pore space as residual droplets (Rahman et al. 2016). This residual trapping can immobilize significant amounts of CO₂. However, the CO₂ not trapped will continue its migration towards the caprock. The caprock will physically trap CO₂, preventing it from migrating to the surface. In the longer term, significant amounts of the residual and physically trapped CO₂ will dissolve in the formation brine. At the interface between dry CO₂ and caprock, CO₂ can enter and dissolve water from the caprock clays (Gaus 2010; Loganathan et al. 2018). This could induce swelling or shrinkage and alter the overall pore structure of the caprock. Clay mineral adsorption of CO₂ traps CO₂, but the swelling pressure can change local stresses within the formation and cause shear failure (Busch et al. 2016).

When CO₂ dissolves in the formation brine it no longer exists as a separate phase, and the buoyancy forces are eliminated. Dissolution of CO₂ is a trigger of geological reactions

due to the formation of carbonic acid (H₂CO₃), see reaction (1).



Carbonic acid will further dissociate into carbonic (CO₃²⁻), bicarbonate (HCO₃⁻) and hydrogen (H⁺) ions (Greenwood and Earnshaw 2012). This causes a decrease in pH of the reservoir brine, which can alter the composition of the caprock matrix. Components susceptible to carbonic acid effects can be dissolved and washed out if carbonic acid diffuses into the pore space of caprocks (Cerasi et al. 2017). Shales usually have very varied mineralogical composition, but are often comprised of quartz, clay minerals, carbonates, feldspar, and organic matter (Shaw and Weaver 1965). Carbonates like calcite, dolomite and siderite are very vulnerable to an acid attack, and a significant reduction of pH will lead to the following reaction:



where X represents a metal ion. Reaction (2) results in a dissolution of the carbonate, which not only changes the mineralogical composition of the rock but can also affect the mechanical and hydrological properties (Gaus 2010).

2 Experimental Method

Conventional laboratory tests are expensive and time-consuming as shale is a difficult material to test. Since shales are low permeable rocks, exposure methods will benefit from using techniques suitable for small samples. Hence a method to obtain fast evaluation of shale properties was developed.

The Draupne formation was used in this study, which is a typical caprock shale. The field core used in the following experiments were from a depth of 2574.9 m (vertical well). The core was made available for research purposes by Equinor and is kept at NGI in Oslo. A few small sections were cut from it and shipped to Trondheim, to be used for mechanical characterisation and exposure to CO₂ at SINTEF. A higher permeability and lower tensile strength have been observed along bedding planes, compared to across bedding (Skurtveit et al. 2015), highlighting the anisotropic nature of this formation.

2.1 Sample Preparation

The Draupne shale was prepared for testing using a scalpel to cut thin disks from cylindrical core plug samples with a diameter of 15 mm. All shale samples were oriented with bedding plane normal parallel to cylinder axis. The disks were then hand grinded with abrasive paper to ensure parallelism of the end surfaces. This approach makes it possible

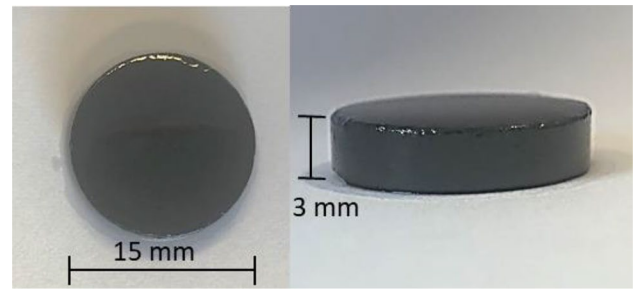


Fig. 1 Picture of a sample after preparation

Table 1 Information about temperature, pressure, and solution for the different exposure conditions

Fluid	Temperature	Pressure	Solution
Brine	Room temperature	Room pressure	1 M NaCl
CO ₂ gas dissolved in brine	Room temperature	30 bar	1 M NaCl
ScCO ₂ dissolved in brine	42 °C	80 bar	1 M NaCl
Dry CO ₂	Room temperature	30 bar	No
Dry ScCO ₂	42 °C	80 bar	No
Air	Room temperature	Room pressure	No

to produce finely grained samples of mm thickness within minutes. The final thickness of the samples ranged between 2 and 4 mm, see Fig. 1. Before, during and after preparation, samples were kept moist using a high viscosity inert laboratory oil (Marcol™ 82). This, to prevent sample desiccation and exposure to air. Before exposure to the different experimental fluids, excess oil was removed by carefully cleaning the samples with a dry cloth. A total of 57 samples were prepared, and to obtain statistics three samples were tested for each condition (exposure fluid and exposure time). Exposure to the different fluids started immediately after the sample preparation was completed. The samples used as references were tested the same day as sample preparation.

2.2 Fluids

Draupne shale samples were exposed to six different fluid conditions: brine, CO₂ gas dissolved in brine, supercritical CO₂ (ScCO₂) dissolved in brine, dry CO₂, dry ScCO₂ and no exposure fluid (air). Reference samples were also tested to obtain data representing initial values. See Table 1 for information regarding each condition. For each exposure fluid studied, nine shale samples were added into a batch test. Three samples were subtracted from the fluids for each predetermined test time and mechanical tests were conducted after 1, 2 and 7 days of exposure. The number of days of exposure was chosen on the basis of previous experiments

with a different type of shale, where the most significant changes in strength occurred within the first 48 h.

All samples were exposed to the different fluids in such a manner that the fluid could diffuse into the samples from all directions (meaning without confinement). The samples exposed to brine solution were stored in a closed container, while the samples exposed to air were left to dry in open air. For the experiments involving gaseous CO₂ (dry CO₂ and CO₂-saturated brine), the gas pressure was set to 30 bar under room temperature. Experiments with ScCO₂ (dry ScCO₂ and ScCO₂-saturated brine) were conducted in a cell able to regulate the temperature. The temperature was set to 42 °C and the system was pressurized to 80 bar to achieve supercritical state. For CO₂-saturated brine solution (gaseous and supercritical), half of the cell was filled with brine before injecting CO₂ and obtaining the desired pressure.

2.3 P-wave Velocity Measurement

P-wave can be used to investigate changes in pore fluid and overpressure of a shale sample (e.g., Prasad 2002; Hamada 2004). The P-wave velocity (v) can be linked to elastic moduli and density (ρ) of the rock by Eq. (3).

$$v = \sqrt{\frac{K + \frac{4}{3}G}{\rho}} \quad (3)$$

where K and G are the undrained bulk and shear moduli of the sample. The undrained bulk modulus is linked to frame (drained) modulus (K_{fr}), fluid modulus (K_f), grain modulus (K_s) and porosity (ϕ) through the Biot–Gassmann Eq. (4) to model fluid substitution.

$$K = K_{fr} + \frac{k_f}{\phi} \frac{\left(1 - \frac{K_{fr}}{K_s}\right)}{1 + \frac{K_f}{\phi K_s} \left(1 - \phi - \frac{K_{fr}}{K_s}\right)} \quad (4)$$

Continuous wave technique (CWT), a method designed to perform measurements on cuttings, was used to measure acoustic velocities of the studied Draupne shale samples. This is a non-destructive technique meaning that after CWT testing, the same sample can be used for further strength measurements. Therefore, acoustic velocity and shear strength were measured consecutively for each sample.

The system is based on a simple CW transmission spectrometer that clamps the sample with oppositely mounted acoustic transducers, thus constituting a composite resonator (Nes et al. 1998). One transducer generates acoustic waves, while the other one detects the signal. The ultrasonic standing wave resonance in the composite resonator is generated by sweeping the excitation frequency of a range of several corresponding standing wave resonances, see Table 2 for inputs used in this experiment. To generate the requested

Table 2 CWT initial inputs

Initial values	Value
Start frequency	1 MHz
Stop frequency	7 MHz
Excitation voltage	10 V
Amplification	50 dB

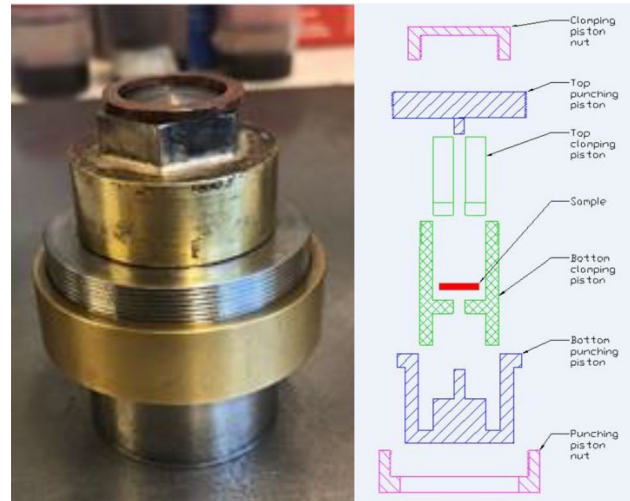


Fig. 2 Picture of the assembled punching tool (left) and schematic illustration presenting the different parts of the punching tool (Stenebraten et al. 2008)

frequency sweep, a frequency generator is used. The receiving transducer detects an amplitude modulated signal containing a resonance curve with resonance peaks. The resonance curve is displayed by a software (Nes et al. 1998) and the neighbouring resonance peaks are picked by the operator, and the velocities are calculated using Eq. (5)

$$v = 2L\Delta f, \quad (5)$$

where v is the p-wave velocity, L is the sample thickness, and Δf is the excitation frequency.

2.4 Shear Strength Test

A punching tool was used to measure the shear strength. This is a mechanical device designed for small samples, like cuttings. The sample disk is held between two clamping pistons (Stenebraten et al. 2008), see Fig. 2.

These clamping pistons have a centred hole where a punching piston can be fitted from each side of the sample. The clamping and punching pistons are locked together in pairs. If an axial load is placed on the punching tool, a shearing force will be exerted onto the sample because the clamping and punching pistons will be forced in opposite

directions. To apply an external force, an MTS load frame with 10 kN capacity was used. The rate of deformation was a predetermined value set as a fixed rate equal to 0.15 mm/min. The axial force was exerted continuously onto the punching tool until failure was detected. The shear strength was measured as the peak force required to create a hole through the sample, divided by the area of the cylindrical cut. Three samples were used to calculate the shear strength for each exposure fluid and time.

2.5 Scanning Electron Microscopy (SEM)

A unique procedure was established to observe the changes in sample surface by taking images and performing elemental mapping of the exact same location on the sample surface, pre- and post-exposure tests. Scanning electron microscopy (SEM) was used to visualize surfaces of shale samples before and after the exposure to different solutions of CO₂ and brine. A Hitachi S-3400 N microscope was used at variable accelerating voltages. Images were acquired with a backscattered electron (BSE) detector. Elemental maps were acquired using energy-dispersive X-ray spectroscopy (EDX). The elemental maps are not quantitative, but show regions (e.g., particles) that are rich in the given element relative to the surroundings. Images and elemental mapping were acquired at the sample surface before it was exposed to any fluid and repeated after 7 days of exposure. It was made sure that the exact same location of the surface was investigated. Since samples needed to be exposed to different fluids after the first SEM imaging, the sample surface was not coated. The samples used in this SEM–EDX procedure did not undergo any other tests.

2.6 X-ray Diffraction (XRD)

X-ray diffraction was used to measure the mineralogical composition of both reference sample (untreated) and treated samples of Draupne shale. A Bruker D8 Advance DaVinci X-ray diffractometer with Bragg–Brentano geometry using CuK α radiation ($\lambda = 1.54187 \text{ \AA}$) was used to measure the mineralogical composition. All the samples were crushed into smaller pieces and dried overnight at room temperature. About 2 g of representative dried samples were grounded into silt-sized particles. Back loading sample preparation was used to avoid any preferred orientation of the constituents. The samples were scanned from 2 to 55° 2 θ . The data analysis does not include amorphous material as e.g., organic material. The method is therefore considered as semi-quantitative analysis. Measurement uncertainty can be due to sample preparation, high background signal. Generally, the uncertainty is relatively larger for smaller peaks. Only bulk mineral XRD was performed in this work.

2.7 Petrophysical Properties

Mercury porosimetry and BET surface area measurement was conducted at MCA services, UK. Mercury porosimetry provides the pore diameter, bulk and grain densities, porosity, and pore throat size distribution. The analysis revealed that the porosity was 9.5%, average pore diameter was 10 nm, bulk and grain densities were 1.9 g/cc and 2.08 g/cc, respectively. The degree of brine saturation was approximately 0.6. Pore throat distribution shows that about 12% of the pore size diameters were larger than 0.1 μm . The measured BET surface area was 10.41 m²/g.

3 Results and Discussion

Experiments have been conducted on small samples of Draupne shale to understand how different exposure fluids affect the shear strength, p-wave velocity, and mineral composition of the shale. The different fluids tested were sodium chloride brine, CO₂ gas dissolved in brine, ScCO₂ dissolved in brine, dry CO₂, dry ScCO₂ and no exposure fluid (air).

3.1 Scanning Electron Microscopy (SEM)

In the literature, SEM is used to track surface changes due to exposure using two different sample surfaces (e.g., Lyu et al. 2016). This introduces complications in interpretation of the observed results since mineral composition can vary between shale samples. To avoid such problems, SEM imaging was done on the same sample before and after exposure tests to observe the change in chemical properties on the sample surface.

A salt layer coated the samples exposed to brine, which can be seen from Fig. 3 where the amount of Na and Cl has increased significantly. A change in chemical composition is only observed for the sample exposed to the combination of brine and CO₂ (gaseous or supercritical state). The samples exposed only to brine or dry CO₂ (gas and supercritical) do not show any significant change in chemical composition on the sample surfaces. SEM images of the sample exposed to gaseous CO₂ are investigated but no image is acquired yet, therefore not included in this work. A series of images showing the sample surfaces before and after exposure tests are presented in Figs. 3, 4, 5, 6.

When CO₂ is dissolved in brine the solution becomes acidic (Greenwood and Earnshaw 2012). An acidic solution can alter the mineral composition, mainly on carbonate minerals (e.g., Bhuiyan et al. 2020). This was reflected in the results, where SEM analysis revealed that no changes in chemical composition were observed on the sample surface

Fig. 3 Elemental mapping of sample surface before and after exposed to brine solution for 7 days

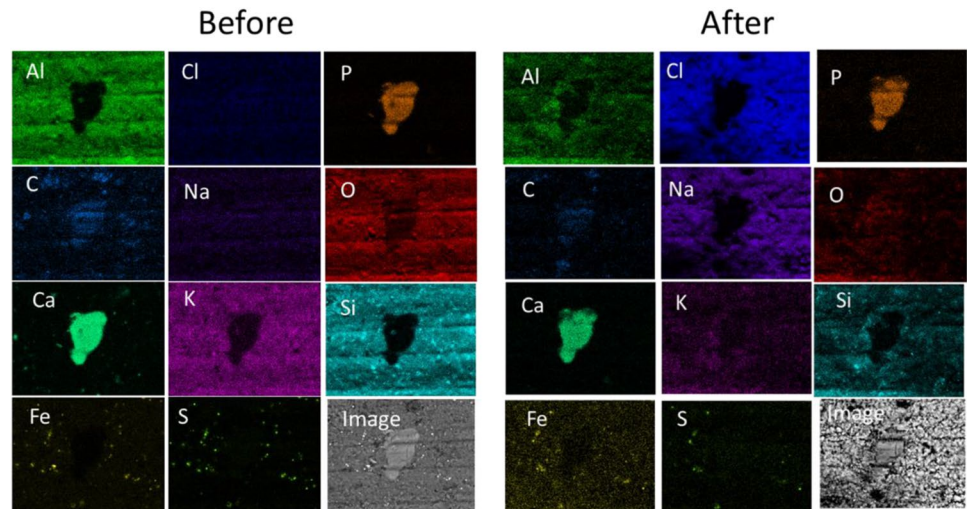


Fig. 4 Elemental mapping of sample surface before and after exposed to CO_2 gas saturated brine solution for 7 days. There is less Ca observed after exposure

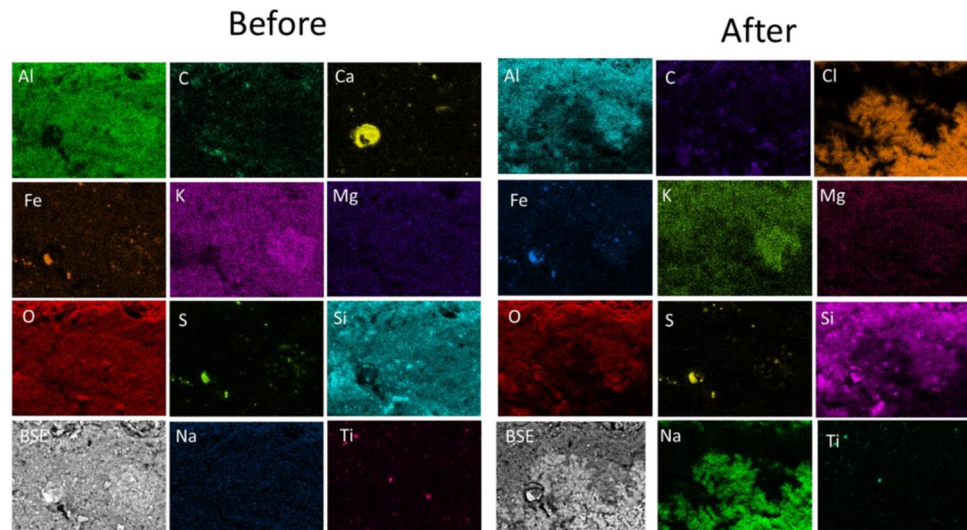


Fig. 5 Elemental mapping of sample surface before and after exposed to dry supercritical CO_2 solution for 7 days. No significant change of elemental composition is observed on the sample surface upon exposure to supercritical CO_2

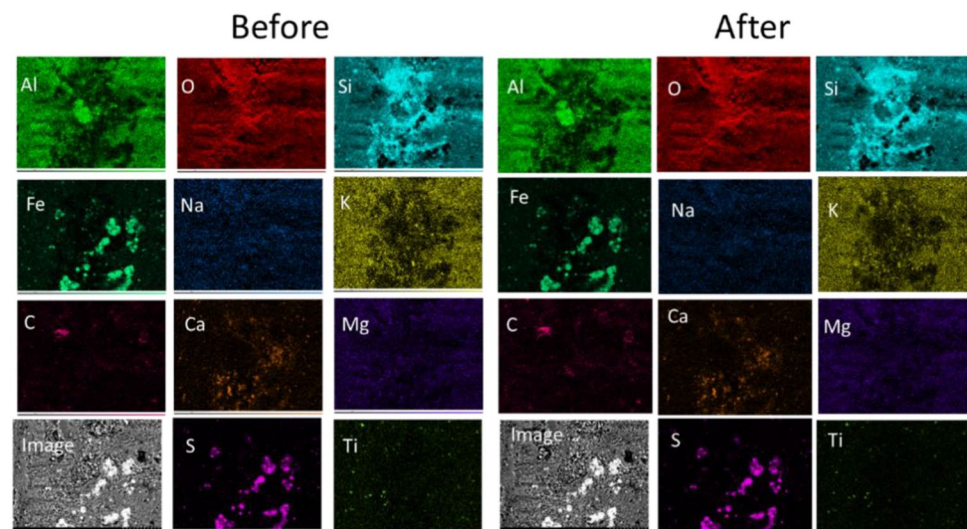
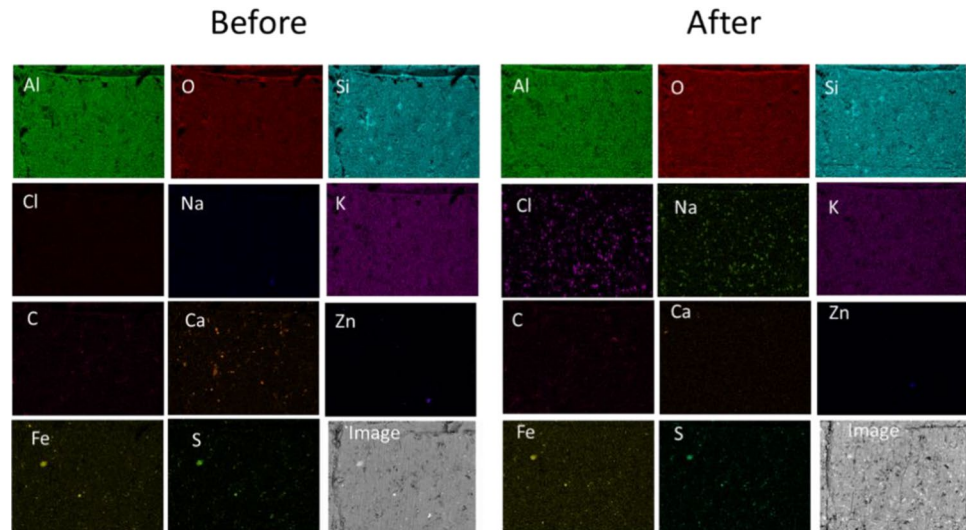


Fig. 6 Elemental mapping of sample surface before and after exposed to supercritical CO₂ saturated brine solution for 7 days. There is less Ca observed after exposure



for the sample exposed to dry CO₂. Carbonate mineral disappeared from the sample surfaces (Figs. 4, 6) when the samples were exposed to CO₂ saturated brines.

3.2 X-ray Diffraction (XRD)

The change of mineral content influenced by exposure fluid is shown in Table 3. TOC (Total Organic Carbon) content of the shale is not included in the XRD analysis. However, TOC was measured for the reference sample and the value is 5.4 wt%.

The results described in Table 3 are obtained for different samples of Draupne shale. This means that the table contains underlying differences due to the fact that two samples of shale are not identical. Table 3 shows no significant change in amount of calcite or siderite after exposure to CO₂, but dolomite is reduced when exposed to air, brine, and gaseous CO₂ (brine + CO₂, and dry CO₂). The observed change in chlorite mineral is difficult to explain. No change in mineralogy contradicts the change in composition (compositional maps by SEM) on the surface of the sample exposed to CO₂

saturated brine solution. One of the possible explanations can be that the dissolution occurred only on the surface and not inside the sample. It is difficult to draw any conclusion since the uncertainty associated with XRD analysis can be high enough to conceal the changes, especially low concentration minerals.

3.3 Shear Strength

Force–displacement curves for samples exposed to the different fluids for 24 h are presented in Fig. 7. For shear strength calculations, three samples were tested for each experimental condition; however, the force–displacement plot shows only one sample for each experimental condition. In the plot the force has been divided by the sample thickness to correlate to the shear strength plot (see Fig. 8) more easily.

From the force–displacement curves it is seen that a nearly linear segment is followed by a sharp drop in force which indicates failure. The shear strength was calculated

Table 3 Description of mineral content for Draupne shale samples exposed to different fluids

	Reference	Air dry	Brine	Brine + CO ₂	Dry CO ₂	ScrCO ₂	Brine + ScrCO ₂
Quartz	15.1	13.9	13.7	14.5	14.7	18.4	16.8
Feldspar	5.7	3.5	4.1	4.6	4.9	5.6	6.9
Kaolinite	16.7	18.0	16.9	19.7	18.7	15.8	16.6
Chlorite	2.3	0	0	0	0	0	0
Mica/illite	13.6	15.9	12.7	14.1	14.5	17.8	19.4
Mixed layer + smectite	42.9	45.4	45.7	43.8	42.1	37.3	35.3
Calcite	0.8	0.7	2.1	0.5	1.4	0.6	0.4
Siderite	0.2	0.3	0.2	0.4	0.4	0.3	0.3
Dolomite/ankerite	0.6	0.0	0.0	0.0	0.0	0.9	0.5
Pyrite	2.1	2.3	4.6	2.3	3.4	3.4	3.8

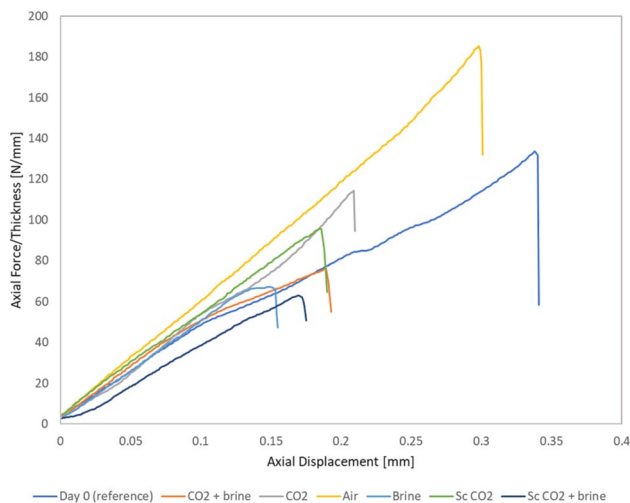


Fig. 7 Force–displacement curves for one sample from each exposure test. The samples were tested after 24 h of exposure. The force has been divided on sample thickness

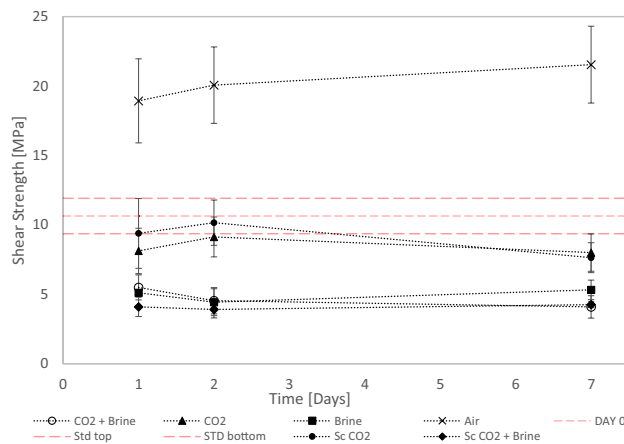


Fig. 8 Plot of average shear strength versus exposure time for Draupne shale samples. The middle horizontal line represents share strength of reference sample (no exposure, day 0) with corresponding standard deviation (upper and lower line). The different exposure fluids tested was CO_2 +brine (white circle), dry CO_2 gas (black triangle), brine solution (black square), air (black cross), ScCO_2 (black circle) and ScCO_2 +brine (black rhombus). The error bars indicate the standard deviation obtained using three samples to calculate the averages

by dividing the maximum force required to break the sample by the area of the cylindrical cut.

Shear strength was measured after 1, 2, and 7 days of exposure, see Fig. 8. The plot represents average shear strength and standard deviations are therefore included.

From the plot in Fig. 8 it is seen that exposing the samples to air led to an increase in shear strength compared to the reference sample, and any other samples tested in this study. This is not uncommon in high permeability sandstone formations, where complete drying is accompanied by a

significant increase in strength (Papamichos 2016). For the Draupne shale, this clearly indicates that the fluid exposure made the sample weaker, especially under exposure to brine solutions. The pore fluid in the cored sample is partly lost on recovery due to outgassing as the sample depressurizes from its in-situ condition to the surface (Dewhurst et al. 2020). Therefore, it is believed that the Draupne shale was not fully saturated before exposure to different fluids. Undersaturated shales can attract fluid into the rock matrix when encountering other fluids (Ewy 2014). If exposed to brine, even if the water activity of the brine is low, the result can still be softening of the rock. This means that the clays in the rock samples will absorb water which causes shale swelling. Similar softening effect was mentioned by Li et al. 2016, where they observed a reduction of UCS and Young's modulus with increase in water content. Khazanehdari and Sothcott 2003, reported a reduction of shear modulus upon water and brine saturation. As most of the softening is believed to be due to adsorption of water, osmotic forces may play a minor role as well. A number of recent studies show the capability of clay minerals (e.g., smectite) to absorb considerable amounts of CO_2 which leads to volumetric expansion, hence reduction of shear strength (Busch et al. 2016). On the other hand, this may also indicate that drying will have the opposite effect, leading to an increase of strength for the samples exposed to air (Szewczyk et al. 2018).

The shear strength of the samples exposed to dry CO_2 (both gas and supercritical) is higher compared to what is observed with samples exposed to dissolved CO_2 (gas or supercritical) or pure brine solution. A slight decrease in shear strength is observed with time (in this case after 7 days) for the samples exposed to dry CO_2 . However, there may be several mechanisms playing a role which may help understanding the differences in the shear strength softening effect upon exposure to different fluids (different states of CO_2 and their mixture with brine). As mentioned, the Draupne shale contains clay minerals that can adsorb fluids such as CO_2 , brine, and their mixtures. It is clear from Fig. 8 that shear strength varies with different fluid exposures. The possible mechanisms of interactions between shale and dry CO_2 , as well as CO_2 dissolved in brine solutions, are summarized in several literature reviews (e.g., Bhuiyan et al. 2020), and described as a) drying and precipitation of salt in pore space due to interaction between dry CO_2 and pore fluid, which can potentially clog the pore matrix. This may lead to change in the rock structure such as shrinkage and cracking within the shale matrix (Feng et al. 2019). However, since the permeability of shale rocks is very low, clogging would most likely make a greater difference if there were fractures in the shale samples. It is also reported that the gaseous CO_2 results in larger salt precipitation compared to supercritical CO_2 (e.g., Miri and Hellevang 2016). A second mechanism is b) sorption of CO_2 in shales, which is well reported in

several articles (e.g., Gensterblum et al. 2014). The magnitude of swelling is different for different shales which can be attributed to stiffness of the shale matrix (the higher the stiffness, the lower the swelling) (Heller and Zoback 2014). In this study the drying and precipitation mechanism were probably overridden by the effect of sorption of CO₂ in the shale, which reduced the shear strength of the samples exposed to dry CO₂. The slow reduction of shear strength (only significant after 7 days of exposure) indicates that the CO₂ sorption mechanism is increasing with longer exposure time. Mineral dissolution mechanisms can be ruled out in this case since the SEM images showed no change in elemental composition.

Figure 8 also shows that the shear strength of the sample exposed to CO₂-saturated brine is lower than for the sample exposed to the dry CO₂. One of the mechanisms to explain the observations is pH effect. In these experiments, the pH effect can only occur when CO₂ is dissolved in brine, which makes the solution acidic (Greenwood and Earnshaw 2012). The samples exposed to CO₂ (gas or supercritical) saturated brines were not significantly different from each other, nor different from the ones exposed to brine solution. Regarding the brine, shear strength softening is most likely due to sorption or suction of brine, which leads to swelling. Swelling decreases the strength of the shale (Lyu et al. 2015). No significant difference between the samples exposed to brine and the samples exposed to CO₂ saturated brine were observed. This suggests that brine is the main component responsible for the strength reduction, and the acidic effects may not be significant for Draupne shale during 7 days of exposure. The dissolution of calcite minerals, as seen in Table 3, probably occurs only on the sample surface, and not inside the sample. This can be supported by the XRD data, with no evidence of significant mineral dissolution.

3.4 P-wave Velocity

The P-wave velocity was measured after 1, 2, and 7 days of exposure. The plot represents average velocities and includes standard deviations. The change in velocity is presented in Fig. 9. For samples exposed to ScCO₂ and ScCO₂-brine solution, acoustic measurements were not feasible. It was not possible to construct a resonance plot thus not possible to calculate the velocity. A potential explanation for this is that the ScCO₂ expanded the clay layers within the shale, causing an attenuation so great that CWT was ineffective.

All samples experience a decrease in P-wave velocity after being immersed in the different fluids. For all samples, except for the samples exposed to dry CO₂ gas, the change in velocity occurs during the first 24 h of exposure. For the dry CO₂ gas, the change is rather slow compared to the other fluids. During the first 24 h of exposure, no significant change within P-wave velocity was observed. A significant change

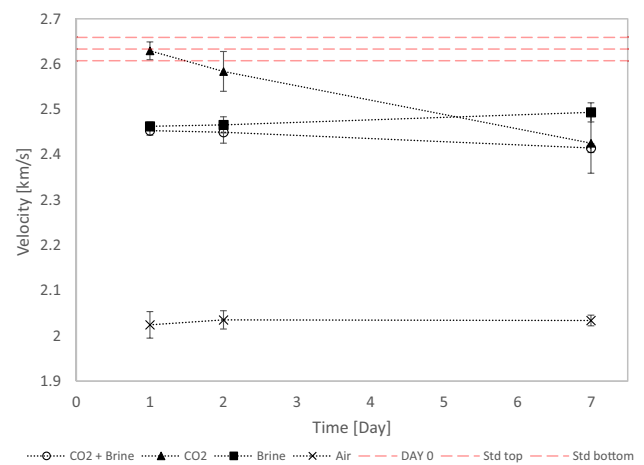


Fig. 9 Plot of average P-wave velocity versus exposure time for Draupne shale samples. The middle horizontal line represents share strength of reference sample (no exposure, day 0) with corresponding standard deviation (upper and lower line). The different exposure fluids tested was CO₂+brine (white circle), dry CO₂ gas (black triangle), brine solution (black square) and air (black cross). The error bars indicate the standard deviation obtained using three samples to calculate the averages

does not happen before 48 h of exposure. The change is most likely related to the slow diffusion of CO₂ gas into the sample, which leads to an increase in drying volume of the sample with time. The P-wave velocity was lowest for the samples that had been exposed to air, in other words dried. A similar observation is made by Szewczyk et al. 2018 who reported lower P-wave velocity for oven dried Mancos shale compared to samples with more than 40% saturation. The reason of lower velocity for air dried samples can be explained by Eq. (3) and (4) in the experimental method section. According to Eq. (4), the bulk modulus of the air-dried sample (no fluid) is equal to the frame modulus which is usually significantly lower than undrained bulk modulus. The velocity for samples saturated with brine and CO₂ saturated brine were higher compared to air dried samples, but still lower than the reference samples. As mentioned earlier, the Draupne shale was undersaturated prior to testing, but with exposure to brine or CO₂ saturated brine the saturation level increased. This means that slightly undersaturated shales show higher velocity than a fully saturated shale. A similar trend was observed by Szewczyk et al. 2018 who obtained higher velocity for a sample with 86% saturation compared to 100% or fully saturated shale.

Summarizing the observations from both shear strength and P-wave velocity, it can be possible to differentiate the acting processes that occurred due to exposure of Draupne shale to different fluids. The effect of drying is significant on shale samples which is supported by the significantly higher shear strength and lower P-wave velocity. When samples are exposed to dry CO₂ (gaseous and supercritical

CO₂) slight reductions in strength and P-wave velocity indicate the drying process is overridden by the sorption effect which softens the shale frame. No change in chemical composition for samples exposed to dry CO₂ is an indication that the softening effect may only depend on the CO₂ sorption which may lead to swelling of the shale's clay minerals. The scenario is very different when Draupne shale comes into contact with brine or CO₂ saturated brine solution. Significant reduction of shear strength and moderate reduction in P-wave velocity are observed. However, there are no significant differences in shear strength and P-wave velocity between the samples exposed to brine or CO₂-saturated brine. This indicates that the brine softening effect is the primary mechanism for reduction of above-mentioned properties. However other processes such as chemical dissolution, absorption of CO₂ cannot be ruled out, but the influence of these mechanisms may be insignificant.

4 Conclusion

The motivation for this study was to investigate whether injected CO₂ in contact with a caprock could alter the caprock's mechanical properties and hence increase the risk of CO₂ leakage. A systematic exposure study was conducted to obtain more insight into the different mechanisms susceptible of changing the shale's properties. The different exposure fluids were chosen to (i) separate the effect of drying from CO₂ sorption, and (ii) separate the effect of softening from the effect of pH. Experiments were conducted on mm-sized disk samples of Draupne shale, reducing fluid diffusion time into the sample. SEM imaging revealed that carbonate minerals disappeared from the sample surface when samples were exposed to CO₂ saturated brines. From shear strength tests it was seen that the samples exposed to brine solutions had the greatest decrease in strength. No significant difference between the samples exposed to brine and the samples exposed to CO₂ saturated brine were observed. This indicates that swelling is the main component responsible for strength reduction in Draupne shale, and the acidic effects may not be significant during 7 days of exposure. This statement is supported by the XRD data, implying no significant mineral dissolution. All samples showed a reduction in p-wave velocity.

Acknowledgements This publication has been produced with support from the Research Council of Norway in the framework of the CLIMIT programme's SPHINCSS—Stress Path and Hysteresis effects on Integrity of CO₂ Storage Site Researcher Project # 268445. The experiments were performed at the Formation Physics Laboratory of SINTEF Industry.

Funding Open access funding provided by SINTEF AS.

Open Access This article is licensed under a Creative Commons Attribution 4.0 International License, which permits use, sharing, adaptation, distribution and reproduction in any medium or format, as long as you give appropriate credit to the original author(s) and the source, provide a link to the Creative Commons licence, and indicate if changes were made. The images or other third party material in this article are included in the article's Creative Commons licence, unless indicated otherwise in a credit line to the material. If material is not included in the article's Creative Commons licence and your intended use is not permitted by statutory regulation or exceeds the permitted use, you will need to obtain permission directly from the copyright holder. To view a copy of this licence, visit <http://creativecommons.org/licenses/by/4.0/>.

References

- Agofack N, Cerasi P, Stroisz A, Rørheim S (2019) Sorption of CO₂ and Integrity of a caprock shale. In: 53rd US Rock mechanics/geomechanics symposium. American Rock Mechanics Association
- Al-Ameri WA, Abdulraheem A, Mahmoud M (2016) Long-term effects of CO₂ sequestration on rock mechanical properties. *J Energy Resour Technol* 138:1
- Benson SM, Cole DR (2008) CO₂ sequestration in deep sedimentary formations. *Elements* 4:325–331
- Bhuiyan MH, Agofack N, Gawel KM, Cerasi PR (2020) Micro- and macroscale consequences of interactions between CO₂ and shale rocks. *Energies* 13:1167
- Briševac Z, Kujundžić T, Čajić S (2015) Current cognition of rock tensile strength testing by Brazilian test. *Rud Geol Naft Zb* 30:101–128
- Busch A, Amann-Hildenbrand A, Bertier P, Waschbuesch M, Krooss BM (2010) The significance of caprock sealing integrity for CO₂ storage. In: SPE international conference on CO₂ capture, storage, and utilization. Society of Petroleum Engineers
- Busch A, Bertier P, Gensterblum Y, Rother G, Spiers CJ, Zhang M, Wentinck HM (2016) On sorption and swelling of CO₂ in clays. *Geomech Geophys Geo-Energy Geo-Resour* 2:111–130
- Cerasi P, Lund E, Kleiven ML, Stroisz A, Pradhan S, Kjølner C, Frykman P, Fjær E (2017) Shale creep as leakage healing mechanism in CO₂ sequestration. *Energy Proced* 114:3096–3112
- Cosgrove JW (1995) The expression of hydraulic fracturing in rocks and sediments. *Geol Soc Lond Spec Publ* 92:187–196
- Dewhurst DN, Raven MD, Shah SSBM, Ali SSBM, Giwelli A, Firms S, Josh M, White C (2020) Interaction of super-critical CO₂ with mudrocks: impact on composition and mechanical properties. *Int J Greenh Gas Control* 102:103163
- Ewy RT (2014) Shale swelling/shrinkage and water content change due to imposed suction and due to direct brine contact. *Acta Geotech* 9:869–886
- Feng G, Kang Y, Sun Z, Wang X, Hu Y (2019) Effects of supercritical CO₂ adsorption on the mechanical characteristics and failure mechanisms of shale. *Energy* 173:870–882
- Fjær E, Holt RM, Raaen AM, Horsrud P (2008) Petroleum related rock mechanics. Elsevier, Amsterdam
- Flett MA, Gurtun RM, Taggart IJ (2005) Heterogeneous saline formations: long-term benefits for geo-sequestration of greenhouse gases. *Greenhouse gas control technologies*, vol 7. Elsevier, Amsterdam, pp 501–509
- Gaus I (2010) Role and impact of CO₂–rock interactions during CO₂ storage in sedimentary rocks. *Int J Greenh Gas Control* 4:73–89

- Gensterblum Y, Busch A, Krooss BM (2014) Molecular concept and experimental evidence of competitive adsorption of H₂O, CO₂ and CH₄ on organic material. *Fuel* 115:581–588
- Greenwood NN, Earnshaw A (2012) *Chemistry of the elements*. Elsevier, Amsterdam
- Hamada GM (2004) Reservoir fluids identification using V_p/V_s ratio? *Oil Gas Sci Technol* 59:649–654
- Hara A, Ohta T, Niwa M, Tanaka S, Banno T (1974) Shear modulus and shear strength of cohesive soils. *Soils Found* 14:1–12
- Heller R, Zoback M (2014) Adsorption of methane and carbon dioxide on gas shale and pure mineral samples. *J Unconv Oil Gas Resour* 8:14–24
- Khazanehdari J, Sothcott J (2003) Variation in dynamic elastic shear modulus of sandstone upon fluid saturation and substitution. *Geophysics* 68:472–481
- Kovscek AR (2002) Screening criteria for CO₂ storage in oil reservoirs. *Pet Sci Technol* 20:841–866
- Li H, Lai B, Lin S (2016) Shale mechanical properties influence factors overview and experimental investigation on water content effects. *J Sustain Energy Eng* 3:275–298
- Loganathan N, Bowers GM, Yazaydin AO, Schaef HT, Loring JS, Kalinichev AG, Kirkpatrick RJ (2018) Clay swelling in dry supercritical carbon dioxide: effects of interlayer cations on the structure, dynamics, and energetics of CO₂ intercalation probed by XRD, NMR, and GCMD simulations. *J Phys Chem C* 122:4391–4402
- Lyu Q, Ranjith PG, Long X, Kang Y, Huang M (2015) A review of shale swelling by water adsorption. *J Nat Gas Sci Eng* 27:1421–1431
- Lyu Q, Ranjith PG, Long X, Ji B (2016) Experimental investigation of mechanical properties of black shales after CO₂-water-rock interaction. *Materials* 9:663
- Masson-Delmotte V, Zha P, Pörtner HO, Roberts D, Skea J, Shukla PR, Pirani A, Moufouma-Okia W, Péan C, Pidcock R, Connors S, Matthews JBR, Chen Y, Zhou X, Gomis MI, Lonnoy E, Maycock T, Tignor M, Waterfield T (2018) IPCC, 2018: Global warming of 1.5 °C (No. IPCC 2018)
- Miri R, Hellevang H (2016) Salt precipitation during CO₂ storage—a review. *Int J Greenh Gas Control* 51:136–147
- Nes O-M, Horsrud P, Sonstebo EF, Holt RM, Ese AM, Okland D, Kjørholt H (1998) Rig site and laboratory use of CWT acoustic velocity measurements on cuttings. *SPE Reserv Eval Eng* 1:282–287
- Nes O-M, Sonstebo EF, Fjær E, Holt RM (2004) Use of small shale samples in borehole stability analysis. In: *Gulf Rocks 2004, the 6th North America rock mechanics symposium (NARMS)*. American Rock Mechanics Association
- Ott H, de Kloe K, Marcelis F, Makurat A (2011) Injection of supercritical CO₂ in brine saturated sandstone: pattern formation during salt precipitation. *Energy Proced* 4:4425–4432
- Papamichos E (2016) Well Strengthening in Gas Wells from near Wellbore Drying. In: *50th US rock mechanics/geomechanics symposium*. American Rock Mechanics Association
- Prasad M (2002) Acoustic measurements in unconsolidated sands at low effective pressure and overpressure detection. *Geophysics* 67:405–412
- Rahman T, Lebedev M, Barifcani A, Iglauer S (2016) Residual trapping of supercritical CO₂ in oil-wet sandstone. *J Colloid Interface Sci* 469:63–68
- Rongved M, Cerasi P (2019) Simulation of stress hysteresis effect on permeability increase risk along a fault. *Energies* 12:3458
- Rubin E, De Coninck H (2005) IPCC special report on carbon dioxide capture and storage. UK Camb. Univ. Press TNO 2004 Cost Curves CO₂ Storage Part 2, 14
- Shaw DB, Weaver CE (1965) The mineralogical composition of shales. *J Sediment Res* 35:213–222
- Skurtveit E, Grande L, Ogebule OY, Gabrielsen RH, Faleide JJ, Mondol NH, Maurer R, Horsrud P (2015) Mechanical testing and sealing capacity of the upper jurassic draupne formation, north sea. In: *49th US Rock mechanics/geomechanics symposium*. American Rock Mechanics Association
- Song J, Zhang D (2013) Comprehensive review of caprock-sealing mechanisms for geologic carbon sequestration. *Environ Sci Technol* 47:9–22
- Stenebraten JF, Sonstebo EF, Lavrov AV, Fjær E, Haaland S (2008) The shale puncher—a compact tool for fast testing of small shale samples. In: *The 42nd US rock mechanics symposium (USRMS)*. American Rock Mechanics Association
- Szewczyk D, Holt RM, Bauer A (2018) The impact of saturation on seismic dispersion in shales—laboratory measurements dispersion in shales—impact of saturation. *Geophysics* 83:MR15–MR34
- Zhang J, Wong T-F, Davis DM (1990) Micromechanics of pressure-induced grain crushing in porous rocks. *J Geophys Res Solid Earth* 95:341–352
- Zhang S, Xian X, Zhou J, Zhang L (2017) Mechanical behaviour of Longmaxi black shale saturated with different fluids: an experimental study. *RSC Adv* 7:42946–42955

Publisher's Note Springer Nature remains neutral with regard to jurisdictional claims in published maps and institutional affiliations.